Performance of Masonry Prisms Filled With Glass Fibre-Reinforced Grout

Gouda, Omar[1]; Hassanein, Ahmed[2], and Galal, Khaled[3]

ABSTRACT

The mechanical properties of the grout and masonry unit control the compressive behaviour of grouted concrete hollow blocks. The grout typically exhibits greater in both the longitudinal and lateral directions when compared to concrete blocks. Hence, a direct consequence is a composite-action incompatibility due to grout-to-block differential strain response under compressive loading. Adding fibres to the grout mixture is expected to affect the compressive strength and ductility of masonry assemblages. The main objective of the current research is to investigate the influence of adding glass fibres to the grout mixture on the compressive stress-strain behaviour of grouted masonry prisms. Glass fibres are expected to enhance the compressive strength, affect the ductility, and control the post-peak behaviour and longitudinal crack propagation. The experimental work involves testing 36 fully grouted half-scaled masonry prisms reinforced with different glass fibres ratios of 0%, 0.03%, 0.06%, and 0.1%; 24 prisms were two blocks high, while 12 prisms were five blocks high. The test specimens were tested concentrically up to failure. The results indicated that the addition of glass fibres to the grout was beneficial to the post-cracking performance and increased the compressive strength of the prisms, hence affecting the compression stress block design of the masonry assemblage.

KEYWORDS: *masonry prisms, fibre reinforced grout, compressive strength, stress-strain behaviour*

[1] Ph.D. candidate, Department of Building, Civil and Environmental Engineering, Concordia University, 1515 St. Catherine West, Montreal, QC, Canada, Omar.Mohamed@concordia.ca

[2] Postdoctoral fellow, Department of Building, Civil and Environmental Engineering, Concordia University, 1515 St. Catherine West, Montreal, QC, Canada, Ahmed.Hassanein@concordia.ca

[3] Professor, Department of Building, Civil and Environmental Engineering, Concordia University, 1515 St. Catherine West, Montreal, QC, Canada, khaled.galal@concordia.ca

INTRODUCTION

Masonry prisms are well recognized for their notably high resistance to compressive forces compared to flexural and tensile forces. Many researchers have emphasized strain incompatibility between the masonry shell and comprised grout in the longitudinal direction [1-6]. This is mainly due to the lower compressive strength capacity of the masonry shell compared to the grout core [7]. Thus, the overall peak stress of the prism is limited to the peak stress of the masonry shell. Researchers also found that incompatibility will occur between the grout and masonry shell when the compressive strength of the grout versus that of the masonry unit is greater than 45% – 50% [8]. Consequently, the grout peak stress is multiplied by a factor less than 1.0 to accommodate such incompatibility for calculating the overall capacity. The rationale behind adding longitudinal and transverse reinforcements to concrete and masonry compression members is increasing the capacity, ductility, and confinement to such members, especially that concrete and masonry are brittle materials.

The reinforcement would also better control the longitudinal and transverse strains. The same concept can be applied to fibres; adding fibres to grouted masonry prisms is expected to enhance the overall ductility. The anticipated confinement should also dominate over the inherent incompatibility of longitudinal and transverse strains - between the grout core and the masonry unit - to yield a significantly enhanced overall mechanical behaviour. Several researchers have studied the potency of adding chopped fibres (steel, glass, natural, etc.) to concrete and its impact on the tensile and flexural behaviour of beams, columns, and shear walls. However, few research efforts exist that deal with the effect of adding fibres to grout on the axial compression behaviour of masonry columns [9-11].

The effect of glass fibres on the behaviour of masonry columns under compression was investigated by Shaheen and Shrive (2007) [12]. In their study, masonry columns were strengthened using sprayed glass fibre reinforced polymers (GFRP) and polyester-based resin. Results showed that this strengthening technique caused a noteworthy enhancement in ultimate strain, a marginal increase in compressive strength, and a decrease in stiffness. In addition to the previous conclusions, the sprayed fibres demonstrated high effectiveness in increasing the strain capacity. Alshugaa (2016) [13] investigated experimentally and numerically the compressive behaviour of hollow block masonry prisms - of two courses constructed in running bond - plastered with steel fibre reinforced mortar (types NS and MS). It was observed that adding steel fibres reduced the cracks at the joints. It was also found that applying a plaster layer on one side only for hollow core concrete blocks is less effective than two sides. The observed failure mechanism was mainly due to buckling of the separated parts and debonding between the plaster and prism. Weng (2009) [14] and Qu et al. (2011) [15] conducted an experimental and numerical analysis for compressive tests on ten plain brick masonry columns. In their study, two columns were control specimens while the remaining eight columns were strengthened with sprayed glass FRP Results demonstrated that the mode of failure changed from brittle to ductile, the ultimate compressive strength increased, and the ductility exhibited notable enhancement due to the confinement effect.

The primary objective of this current research is to study the effect of adding chopped glass fibres with different percentages to normal strength grout. The experimental program includes observing and analyzing the overall stress-strain behaviour, the ultimate capacity, and the ductility of concrete masonry prisms.

EXPERIMENTAL PROGRAM

The experimental program comprises 36 half-scale fully grouted concrete masonry prisms divided into two groups: A and B. All the prisms were tested monotonically under axial compression. Group A includes 24 prisms constructed of two courses with a stack bond of 5 mm mortar between the concrete stretcher units, with a height-to-thickness ratio (h/t) equals 2.06, according to ASTM C1314 [16]. Out of the 24 prisms, 12 prisms were constructed from normal strength stretcher blocks, and the other 12 prisms were of high strength blocks. This choice aims to study the effect of varying block strength. For all the 24 prisms, the cross-section is 185 mm x 90 mm, and the height is 185 mm, as shown in Fig. 1. Group B has 12 normal strength concrete prisms of two-block thickness and five blocks high, constructed in a running bond using 5 mm of mortar. All prisms' cross-section is 185 mm x 185 mm and 470 mm in height, as shown in Fig. 1. The primary variables selected in this study were the strength of the stretcher block, the percentage of glass fibres, and the shape/dimensions of the tested prisms. The five-course prisms were selected to simulate the behaviour of the boundary elements in shear walls; however, the two-course prisms were chosen to represent the standard tested prisms as per ASTM C1314 [16]. The details of the 36 prisms are presented in Table 1.
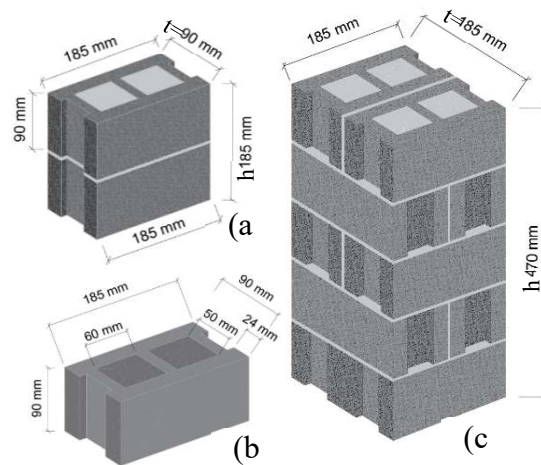
Figure 1: (a) Dimensions of half-scale fully grouted prisms of group A with h/t of 2.06; (b) Typical dimensions of the half-scale block; (c) Dimensions of half-scale fully grouted prisms of group B with h/t of 2.54.

Table 1: Test matrix and properties of prisms

Group	ID	Block strength	Glass fibre percentages (%)	Number of specimens
A	N-C	Normal	-	3
	N-G0.03	Normal	0.03	3
	N-G0.06	Normal	0.06	3
	N-G0.10	Normal	0.10	3
	H-C	High	-	3
	H-G0.03	High	0.03	3
	H-G0.06	High	0.06	3
	H-G0.10	High	0.10	3
B	P-C	Normal	-	3
	P-G0.03	Normal	0.03	3
	P-G0.06	Normal	0.06	3
	P-G0.10	Normal	0.10	3

The prisms were classified into four sets; the first set includes control prisms, and the other three sets comprise the fibre-grouted prisms. The percentages of the glass fibres are 0.03%, 0.06%, and 0.10% of the volume of the total grout mix, wherein each series has three replicates. The glass fibre percentages were selected based on typical mixes found in the literature and recommendations provided by the manufacturer. The recommended dose by the manufacturer is 0.035% of the concrete mixture volume. Each prism from group A is given a notation as X-C/G-Y-#, where X stands for the type of block whether normal, "N", or high strength, "H"; C or G stands for the control or the GFRP specimens; Y is the percentage of glass fibre in each prism, and # stands for the number of the replicate prism in the set, i.e., 1, 2, or 3.

For group B, each prism is notated as P-C/G-Y-#, where P stands for prism. A professional mason constructed the prisms. After setting, the prisms were scrubbed from the inside to remove any dry mortar bumps to avoid any obstructions that may happen during the pouring of grout, which may cause inner cavities inside the grout, subsequently causing a reduction in prism strength. The grout was mixed using an automatic concrete mixer. The guidelines of ACI 544.1R-09 [17] were followed concerning adding fibres to the grout. The fibres were gradually and uniformly distributed into the mixture with caution to prevent any potential fibre clogging.

MATERIAL PROPERTIES

Masonry blocks

The masonry blocks used in constructing the prisms were half-scale stretcher units; typical dimensions of the half-scale block are shown in Fig. 1. According to ASTM C140 [18], three units should be tested in compression to determine the compressive strength. Consequently, three half-scale normal strength blocks and high strength blocks were tested to determine their average compressive strengths and variation (COV) coefficient. Before testing the blocks, the top and bottom surfaces were capped using high-strength white dry-stone material to ensure the uniform

distribution of the load onto the block. According to ASTM C140 [18], the net surface area was estimated with an approximate value of 8668 mm^2 and COV of 1.54%. The average compressive strength of the normal strength stretcher blocks was 24.2 MPa with a COV of 8.9%, whereas the high strength stretcher block's average compressive strength was 34.9 MPa with a COV of 9.5%. According to ASTM C140 [18], three half-scale units were tested to determine the density, moisture content, and absorption. It was reported that the density was 2196 kg/m^3 with COV of 4.03%, the moisture content was 1.21% with COV of 1.11%, and the absorption was 4.85% with COV of 4.53%. All the specimens were stored and tested in the structure laboratory at Concordia University at a steady room temperature of 25Cº.

Mortar

The grouted prisms were constructed by binding the stretcher blocks using a 5 mm thick mortar. The mortar type used was prebagged Type S. The compressive strength of the mortar was determined according to CSA A179-14 [19] procedures, where six 50 mm cubes were tested from each batch. According to CSA A179-14 [19] and ASTM C109-16a [20] recommendations, no special preparations or capping are required for the cubes' testing. The measured average compressive strength of the cubes was 13.2 MPa, with a COV of 9.3%.

Grout

A ready mix, commercially available, 15 MPa grout was used in grouting the prisms. According to CSA A179-14 [19], three cylinders are required to determine the compressive strength for each grout batch. Therefore, a total of 12 cylinders were sampled, i.e., three cylinders per mix. The cylinders were cast in 100 mm diameter and 200 mm height plastic moulds. All cylinders were placed in lab temperature water for curing. The compressive strength was determined by testing one cylinder at 7 days and two cylinders at 28 days, based on the recommendations of CSA A179-14 [19]. Based on the ASTM C1019-14 [21] specifications, the grout core should be tested to evaluate its strength after losing the free water absorbed by the block units. For each grout mixture and block unit strength, three grout core prisms having dimensions of 90 x 90 x 180 mm were prepared by placing the block units in a position that permits the formation of moulds for the grout core. The inner face of the mould was lined with a paper towel as recommended by ASTM C1019-14 [21] to prevent any bonding between the grout core and the block units; the results are displayed in Table 2. A high-strength white dry-stone material was applied as a top and bottom capping, as per ASTM C617-12 [22]. The measured grout compressive strengths are presented in Table 2.

The average compressive strength of the grout cylinders at 7 days for the control cylinders, 0.03%, 0.06%, and 0.10% fibre-percentages were 15.90, 16.74, 17.22, and 17.46 MPa, respectively, while after 28 days, the average strengths were 19.83, 22.06, 23.50, and 24.60, respectively, with a corresponding COV of 8.9%, 1.5%, 6.1%, and 1.2%, respectively. It was found from the test results of the normal strength blocks that the average grout core compressive strengths for the 0%, 0.03%, 0.06%, and 0.10% fibre reinforced grout were 20.86, 22.25, 23.51, and 24.74 MPa, with a coefficient of variation of 4.4%, 5.2%, 7.2%, and 4.0%, respectively. While for the high strength blocks, the compressive strengths for the 0%, 0.03%, 0.06%, and 0.10% fibre reinforced grout

were 19.11, 21.81, 22.83, and 24.62 MPa, with a coefficient of variation of 5.5%, 3.0%, 6.8%, and 3.2%, respectively. The strengths comparison between the of the water retaining grout cylinders and the free water grout moulded core shows that the compressive strength of the grout moulded core is higher than the corresponding grout cylinder, which is conforming to the results of Joyal (2014) [23]; and Mohamed (2018) [24], that is returned to the effect of water loss absorbed by the dry masonry blocks on the contrary to the water retaining cylinders.

Table 2 - Material properties

| Material type	Batch	Ultimate load (kN)	Strength (MPa)	COV (%)	Number of specimens
Normal Strength block	–	210	24.20	8.89	3
High Strength block	–	303.3	34.90	9.50	3
Mortar cubes	–	32.93	13.17	9.33	6
Grout cylinders (100 x 200 mm)	Batch 1 (0% fibres)	155.9	19.85	8.90	3
	Batch 2 (0.03% fibres)	173.3	22.06	1.45	3
	Batch 3 (0.06% fibres)	168.8	21.50	6.08	3
	Batch 4 (0.10% fibres)	185.4	23.60	1.20	3
Grout core moulded (Normal strength block) (90 x 90 x 180 mm)	Batch 1 (0% fibres)	168.97	20.86	4.41	3
	Batch 2 (0.03% fibres)	180.22	22.25	5.23	3
	Batch 3 (0.06% fibres)	190.46	23.51	7.19	3
	Batch 4 (0.10% fibres)	200.40	24.74	3.97	3
Grout core moulded (High strength block) (90 x 90 x 180 mm)	Batch 1 (0% fibres)	154.79	19.11	5.47	3
	Batch 2 (0.03% fibres)	176.66	21.81	2.95	3
	Batch 3 (0.06% fibres)	184.92	22.83	6.77	3
	Batch 4 (0.10% fibres)	199.42	24.62	3.22	3

Glass Fibres

The manufacturer's specifications mentioned that the tensile strength of the fibres was 2050 MPa, while the modulus of elasticity was 74 GPa. The fibres were 19 mm in length and 18 μm in diameter. The density of the fibres was 2.54 g/cm^3, and the manufacturer recommended an optimum amount of 900 grams/m^3 (0.035% of the mixture volume). Consequently, the selected fibre volume percentages were 0.03%, 0.06%, and 0.10%.

Instrumentation and testing

All prisms were capped at the top and bottom, between the prism and the steel plates, using high strength white dry-stone material to ensure that the load is uniformly transferred from the loading cylinder to the prism, as shown in Fig. 2.

The prisms were vertically leveled before capping to prevent any leaning that might affect the results. The prisms were placed under the compression loading cylinder with a capacity of 5000 kN installed under a 6000 kN reaction frame; the prisms were loaded through monotonic concentric compression loading up to failure. A spherical head, capable of moving in any direction, was placed and centred between the loading cylinder and the top steel plate. The dimensions of the spherical plate and steel plates were following the guidelines of the CSA S304-14 [25]. The

concentricity of the test specimens was checked using self-leveling laser devices to ensure the vertical alignment of the prisms and prevent any eccentricity between the loading cylinder, loading plate, and the prisms. Two potentiometers were installed to measure the displacement over the entire height of the prisms, placed at the center of the front and back faces of the prism. The loading protocol and loading rates followed the CSA S304-14 [25] limits. The applied loading type was a monotonic uniaxial compressive load to the prisms up to failure using a loading rate of 0.005 mm/sec. This loading rate was adopted up to an axial strain of 0.002, then decreased to 0.003 mm/sec to capture the post-peak behaviour of the prisms with more accuracy.
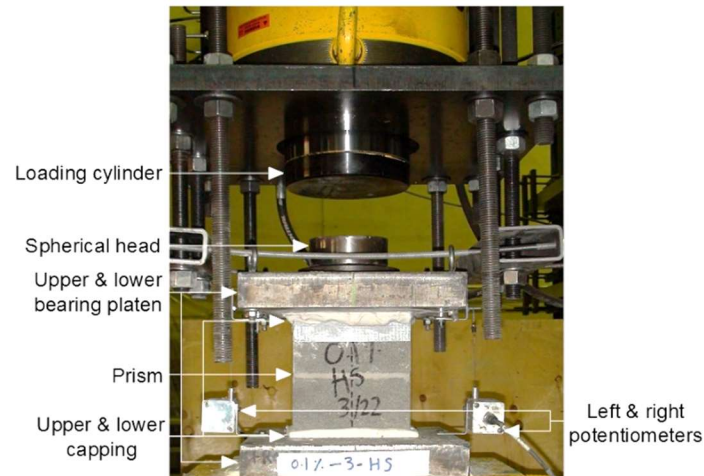

Figure 2: Test setup and instrumentation for the masonry prism.

## RESULTS AND DISCUSSION

Failure mechanism
For the two-course prisms "Group A", the failure mechanism was dominated by shear failure for both the normal and high strength prisms; this is due to the low height-to-thickness ratio and the high brittleness of the stretcher blocks and grout. The failure started by the initiation of diagonal cracks in the face-shell and end webs. Cracks propagated until they reached the mortar and continued propagation in a direction parallel to the mortar, as shown in Fig. 3.

Failure started by spalling the face-shell followed by spalling of the end web, which caused a sudden reduction in the axial stiffness, especially in the control prisms. However, for prisms comprising glass fibres, the stress-strain degradation was gradual in most prisms, especially in the low-fibre percentage prisms and the normal strength prisms. The shear failure also dominated in the glass fibres prisms. The angle of diagonal cracks with the vertical was tending to decrease with increasing the fibre percentage. For the five-course specimens "Group B"; the failure mechanism tended to be splitting by vertical cracks accompanied by some diagonal cracks near the ends, as shown in Fig. 4. The splitting failure can be attributed to the specimen's geometry, which behaves as a column without internal reinforcement resulting in splitting failure.
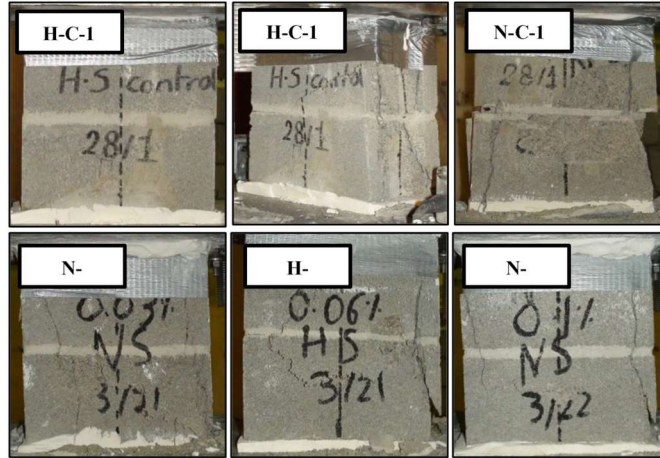
Figure 3: Failure modes of normal and high strength prisms from group A for control and fibre-reinforced grouted prisms.

The crack propagation was similar for prisms with and without glass fibres, which could be attributed to the fact that the fibres – that are entirely comprised within the grout matrix – cannot extend their effect to the concrete block. Herein, the typical failure commenced with the spalling of block parts and ended up with the crushing of the inner grout. The failure was initiated by cracking in the face-shells and end webs, then cracks propagated vertically, followed by spalling of both face-shell and end webs. Subsequently, the grout resisted all applied loads, and the inner cracks within the grout increased until a sudden crushing in the grout occurred.
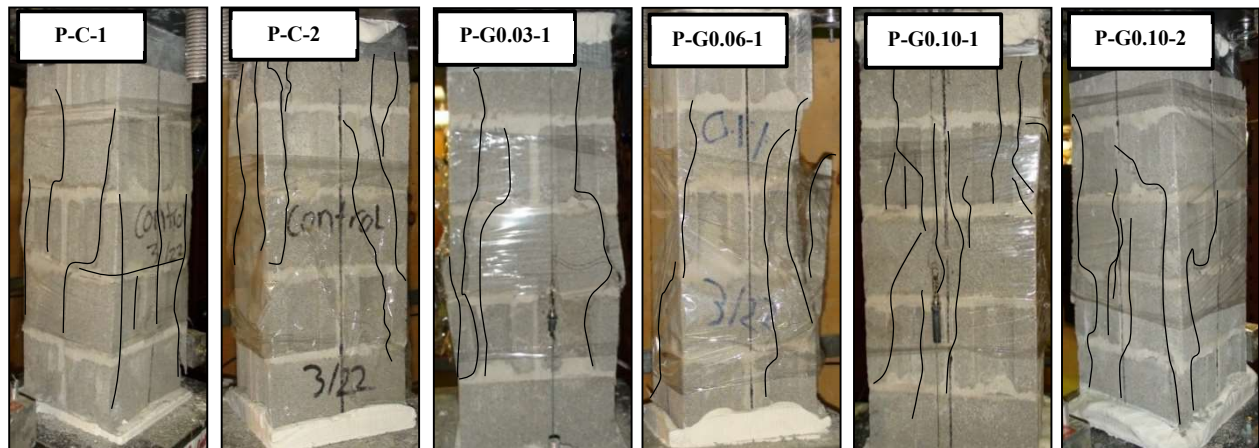

Figure 4: Typical failure modes of prisms from group B for control and fibre-reinforced grouted prisms.

Axial stress-strain relationship

The axial stress is defined as the measured force divided by the total cross-sectional area, including the stretcher block area and the grout area. The area of cross-sections was estimated to be 16291 mm^2 and 33506 mm^2 for group A and group B, respectively. The average strain is calculated by

dividing the average reading of the two potentiometers installed at each side of the prism near the web by the gauge length. Figure 5 shows the axial stress-strain curves of Group A.
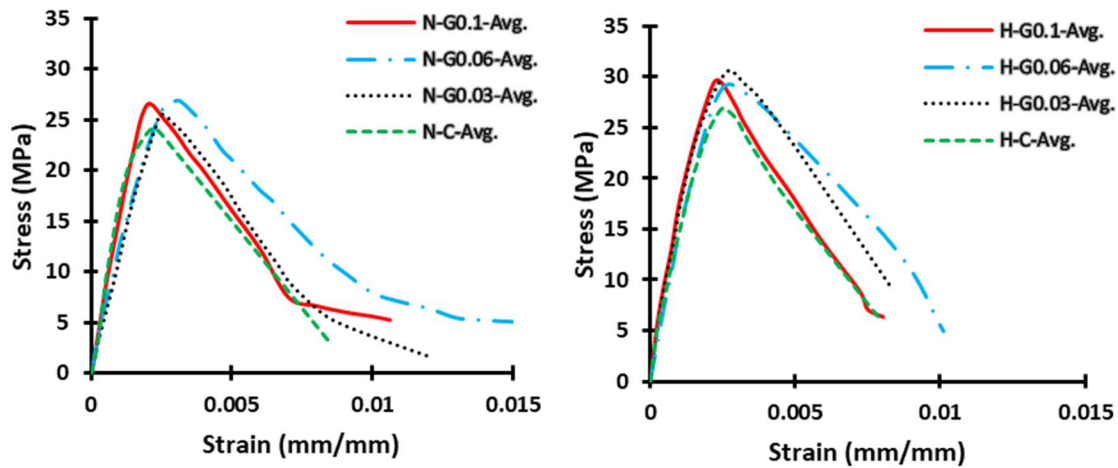
Figure 5: Average axial stress-strain curves of group A prisms.

For this group, which comprises the two-course fully grouted prisms with $h/t = 2.06$, it was observed that the stress-strain curve starts ascendingly with a quasi-parabolic shape. The behaviour is similar to the typically recognized stress-strain relations of masonry prisms, with no deviation in its path. Before reaching the peak strength, the curve deviates due to the loss in stiffness accompanied by cracks propagation in the mortar and face shell until it reaches the peak compressive strength of the prism. Consequently, a descending branch commences due to loss of stiffness, representing the post-peak portion of the curve after prism failure. During the test in the normal and high strength control prisms, it was evident that after attaining the compressive strength, degradation occurs in a rapid sudden-drop manner, causing sudden failure in the specimen. For prisms comprising glass fibres, this sudden drop becomes considerably gradual for normal strength prisms, especially the prisms of grout comprising 0.03% and 0.06% glass fibres. However, for the 0.10% fibre prisms, the abrupt degradation appeared to be less pronounced than that of the control prisms, yet higher than the case of 0.03% and 0.06% fibre comprising prisms. This could be attributed to the fibres' adverse impact on workability if increased, resulting in internal irregular void pockets that cause this abrupt drop in the stress-strain curve. For the high strength prisms, although the descending branch of the stress-strain curve is not sudden as in the control prisms' case, this branch adopts a steeper course than that of normal strength prisms. This is due to the greater brittleness of high strength blocks than normal strength ones, thus affecting the stress-strain behaviour. A higher compressive strength was typically observed for high strength prisms compared to the normal strength counterparts. For the second group (B), which involves five-course normal-strength fully grouted boundary element prisms, with an h/t ratio = 2.54, the stress-strain curves were monitored to display a parabola-like ascending slope with a gradual increase in stiffness. After that, the stiffness started to decrease as a result of the induced cracks in the blocks. After reaching the axial compressive strength and the peak axial strain, a large portion

of the acquired stiffness was lost due to the spalling of the face shells; consequently, the post-peak slope of the curve was accompanied by the deterioration of the inner grout until resistance ceases. The axial stress-strain relations of group B are presented in Figure 6.
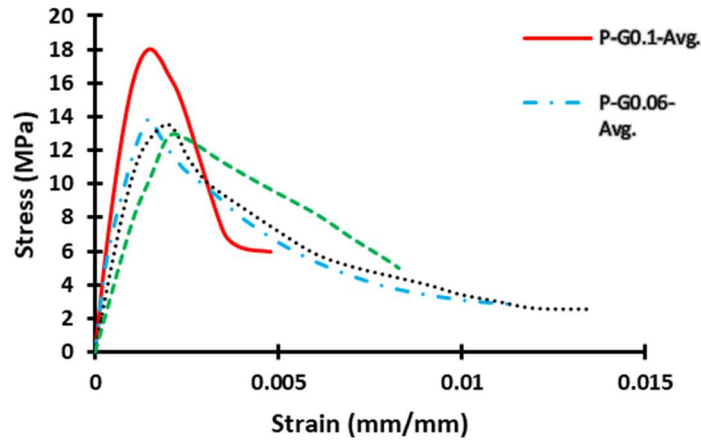
Figure 6: Comparison between the axial stress-strain curves of the control, 0.03%, 0.06%, and 0.10% fibres for prisms of group B.

The degradation branch of each curve was observed to be less steep than that of the two-course prisms. In referral to control specimens, the prisms with glass fibres percentages 0.03% and 0.06% exhibited more degradation. However, the prisms with 0.10% fibre showed gradual degradation of stress-strain curves until 75% of the axial compressive strength, followed by a sudden steep drop in the curve until 25% of the compressive strength. After that, the curve persisted in descending while exhibiting more ductility. The average axial strains were measured for each group. It was observed that by increasing the fibre percentages from 0% up to 0.03%, 0.06%, and 0.10%, the average axial peak strain decreased by 8%, 24%, and 37%, respectively. Herein, the average ultimate strain at 75% of the f'_m decreased by 35%, 52%, and 59%, respectively. Moreover, the average ultimate strain at 50% of the f'_m decreased by 23%, 37%, and 55%, respectively. This shows that the fibres contributed to controlling the axial deformation, within the five-course prisms, by reducing the strains more than the two-course prisms.

CONCLUSIONS
This paper aims at investigating the axial compressive stress-strain behaviour of 36 half-scaled masonry fibre-reinforced grouted prisms with different fibres percentages. The main objective is to study the influence of adding chopped GFRP fibres to the grout mixture on enhancing the performance of the axial compression masonry prisms. The following conclusions were drawn:

1- The dominant mode of failure of the two-course prisms was shear failure accompanied by diagonal cracks. However, splitting failure with vertical cracks controlled the mode of failure of the five-course prisms.
2- For the two-course prisms, the post-peak behaviour was brittle in both the normal and high strength prisms. For the five-course prisms, the post-peak behaviour showed ductile post-peak behaviour in the descending branch.

3- Regarding the normal and high-strength masonry blocks, the fibre reinforced grout enhanced the peak and ultimate strains. However, for the five-course prisms, the peak and ultimate strains decreased by increasing the fibre amount for the three percentages.

4- The addition of glass fibres effectively decreases the rate of degradation in the descending slope of the stress-strain curves for the normal strength prisms, including 0.03% and 0.06% fibres, hence, converting the failure from occurring suddenly to be more gradual.

5- Adding glass fibres to the grout mix did not influence the compressive strength at low fibres percentages; however, its impacts appeared at high percentages (0.10%) by increasing the compressive strength for the prisms in the two- and five-course prisms up to 10% and 39%, respectively. Also, the modulus of elasticity of the prism increases by increasing the glass fibre percentages in the grout.

6- The addition of glass fibres to grout did not overcome the incompatibility between the grout and masonry block. Hence, further research is required to address the high fibres percentages on the compatibility of the masonry assemblages.

REFERENCES

[1] Drysdale RG, Hamid AA. Behavior of Concrete Block Masonry under Axial Compression. Journal of American Concrete Institute, 1979. doi:10.14359/6965.

[2] Romagna RH, Roman HR. Compressive Strength of Grouted and Un-grouted Concrete Block Masonry. Proceedings of the British Masonry Society, 399-404, 2002.

[3] Long L, Hamid A, Drysdale R. Small-scale modelling of concrete masonry using ½ scale units: a preliminary study. 10th Canadian Masonry Symposium, Banff, Alberta, Canada, 2005.

[4] Fortes ES, Parsekian GA, Fonseca FS. Relationship between the compressive strength of concrete masonry and the compressive strength of concrete masonry units. Journal of Materials in Civil Engineering, 2015. doi:10.1061/(ASCE)MT.1943-5533.0001204.

[5] Obaidat AT, Ashour A, Galal K. Stress-Strain Behavior of C-Shaped Confined Concrete Masonry Boundary Elements of Reinforced Masonry Shear Walls. Journal of Structural Engineering (United States), 2018. doi:10.1061/(ASCE)ST.1943-541X.0002120.

[6] Abdelrahman B, Galal K. Influence of pre-wetting, non-shrink grout, and scaling on the compressive strength of grouted concrete masonry prisms. Construction and Building Materials, 2020. doi:10.1016/j.conbuildmat.2019.117985.

[7] Priestley M.J.N., Hon CY. Prediction of Masonry Compression Strength Part:1. New Zealand Concrete Construction Journal, Vol. 28, 11-14, 1984.

[8] Khalaf FM, Hendry AW, Fairbairn DR. Study of the compressive strength of blockwork masonry. ACI. Structural Journal, 1994. doi:10.14359/4139.

[9] S.T. Tassew, A.S. Lubell, Mechanical properties of glass fiber reinforced ceramic concrete, Construction and Building Materials (2014), https://doi.org/10.1016/ j.conbuildmat.2013.10.046.

[10] A.B. Kizilkanat, N. Kabay, V. Akyüncü, S. Chowdhury, A.H. Akça, Mechanical properties and fracture behavior of basalt and glass fiber reinforced concrete: An experimental study, Journal of Construction and Building Materials (2015), https://doi.org/10.1016/j.conbuildmat.2015.10.006.

[11] T. Simões, H. Costa, D. Dias-da-Costa, E. Júlio, Influence of fibres on the mechanical behaviour of fibre reinforced concrete matrixes, Journal of Construction and Building Materials (2017), https://doi.org/10.1016/ j.conbuildmat.2017.01.104.

[12] Shaheen E, Shrive NG. Sprayed glass fibre reinforced polymer masonry columns under concentric and eccentric loading. Canadian Journal of Civil Engineering, 2007. doi:10.1139/L07-069.

[13] Alshugaa M, Rahman MK, Baluch MH, Al-Osta M, Sadoon A. Compressive behavior of hollow block masonry prism plastered with steel fiber reinforced mortar with microsilica and nanosilica.

Brick and Block Masonry: Trends, Innovations, and Challenges - Proceedings of the 16th International Brick and Block Masonry Conference, IBMAC 2016.

[14] Weng R. Research on compressive behavior of unreinforced brick masonry strengthened by SGFRP, M.Sc. thesis, Wuhan University of Technology, 2009.

[15] Gu Q, Peng B, Weng R. Analysis of compressive capacity of brick masonry compressively strengthened with sprayed GFRP. Huanan Ligong Daxue Xuebao/Journal of South China University of Technology (Natural Science) 2011. doi:10.3969/j.issn.1000-565X.2011.04.025.

[16] ASTM C1314. Standard Test Method for Compressive Strength of Masonry Prisms. ASTM International, 2015. doi:10.1520/C1314-14.2.

[17] ACI. Committee 544. Report on Fiber Reinforced Concrete - ACI 544.1R-96 (Reapproved 2009). A.C.I. Manual of Concrete Practice, 2013.

[18] ASTM. C140 Standard Test Methods for Sampling and Testing Concrete Masonry Units and Related Units. American Society for Testing and Materials, 2017. doi:10.1520/C0140.

[19] CSA. A 179-14 (2014), mortar and grout for unit masonry. A179–14, Canadian Standards Association, 2014, Mississauga, ON.

[20] ASTM. C109-16a (2016), Standard Test Method for Compressive Strength of Hydraulic Cement Mortars (Using 2-in . or [50-mm] Cube Specimens) 1. Chemical Analysis. doi:10.1520/C0109.

[21] ASTM. A1019 (2014), Standard Test Method for Sampling and Testing Grout. C1019-14, Astm International. 1–5. doi:10.1520/C1019-11.2.

[22] ASTM C617/C617M − 12. Standard Practice for Capping Cylindrical Concrete Specimens. ASTM International 2012. doi:10.1520/C0617.

[23] Joyal M. Enhanced ductility of masonry shear walls using laterally confined (self-reinforced) concrete block. M.Sc. thesis, McMaster University, 2014.

[24] Mohamed M. Compressive Stress-strain of Unreinforced Masonry Boundary Element Prisms. 2018. M.Sc. thesis, Concordia University.

[25] CSA Design of masonry structures, CSA S304. 2014. Canadian Standards Association, Mississauga, ON.